농학석사학위논문

# Functional Characterization of a Histone Lysine Demethylase Gene in the Rice Blast Fungus, *Magnaporthe oryzae*

# 벼 도열병균의 히스톤 라이신 탈메틸화 효소 유전자의 특성 규명

2014년 2월

서울대학교 대학원

농생명공학부 식물미생물학전공

**허 아 람**

**A THESIS FOR THE DEGREE OF MASTER OF SCIENCE**

# Functional Characterization of a Histone Lysine Demethylase Gene in the Rice Blast Fungus, *Magnaporthe oryzae*

**BY**

**ARAM HUH**

**Department of Agricultural Biotechnology**

**The Graduate School of Seoul National University**

**February 2014**

농학석사학위논문

# 벼 도열병균의 히스톤 라이신 탈메틸화 효소 유전자의 특성 규명

지도교수 이 용 환

이 논문을 농학석사학위논문으로 제출함
2014년 2월

서울대학교 대학원
농생명공학부 식물미생물학전공

허 아 람

허아람의 석사학위논문을 인준함
2014년 2월

위 원 장 김 국 형

부위원장 이 용 환

위 원 이 인 태

A THESIS FOR THE DEGREE OF MASTER OF SCIENCE

# Functional Characterization of a Histone Lysine Demethylase Gene in the Rice Blast Fungus, *Magnaporthe oryzae*

UNDER THE DIRECTION OF DR. YONG-HWAN LEE

SUBMITTED TO THE FACULTY OF THE GRADUATE SCHOOL OF SEOUL NATIONAL UNIVERSITY

BY
ARAM HUH

MAJOR IN PLANT MICROBIOLOGY
DEPARTMENT OF AGRICULTURAL BIOTECHNOLOGY

FEBRUARY 2014

APPROVED AS A QUALIFIED THESIS OF ARAM HUH
FOR THE DEGREE OF MASTER OF SCIENCE
BY THE COMMITTEE MEMBERS

CHAIRMAN Kook-Hyung Kim

VICE CHAIRMAN Yong-Hwan Lee

MEMBER Yin-Won Lee

# ABSTRACT

# Functional Characterization of a Histone Lysine Demethylase Gene in the Rice Blast Fungus, *Magnaporthe oryzae*

Aram Huh

Major in Plant Microbiology

Department of Agriculture Biotechnology

The Graduate School of Seoul National University

The post-translational modification of histones plays important roles in regulating chromatin dynamics and transcription. It has been shown that disruption of proper modifications can lead to developmental defects and cancer in plants and mammals, respectively. Despite the generality of histone modifications as epigenetic mechanism in eukaryotes, implication of histone modifications in fungal pathogenesis is beginning to emerge. To date, two classes of histone demethylases have been identified: LSD and JmjC domain-containing family proteins. Here I reported identification and

characterization of putative histone JmjC demethylases in the model plant pathogenic fungus, *Magnaporthe oryzae*. Combining BLAST and HMMER, seven genes encoding putative JmjC domain-containing histone demethylase were identified and named them as *MoJMJ1* to *MoJMJ7*. Phylogenetic analysis showed that five of them belong to JARID, JMJD2, JHDM2 and JmjC-only domain groups, and the others were predicted to be fungal specific. Deletion of *MoJMJ1*, belonging to JARID group, resulted in defects in vegetative growth, asexual reproduction, autolysis, appressorium formation and invasive growth. The genetic approach was followed by biochemical approaches to examine the demethylase activity and identify target genes affected by steady state level of histone methylation. The expression of the genes, involved in signaling transduction pathways for appressorium development, and other TFs including *MoHOX* genes showed significant changes in Δ*Mojmj1*. Introduction of native *MoJMJ1* gene into Δ*Mojmj1* restored not all but defects in vegetative growth, asexual reproduction, autolysis and appressorium formation, indicating the importance of regulating histone demethylation by *MoJMJ1* during fungal development and appressorium formation. It is anticipated that this work would provide not only the insight into epigenetic regulation of fungal pathogenesis but also the knowledge that can be used in devising new control strategies against rice blast.

**KEYWORDS**: histone demethylase, *Magnaporthe oryzae*, pathogencity, appressorium development

Student number: 2012-21192

# CONTENTS

# LIST OF TABLES

# LIST OF FIGURES

# INTRODUCTION

In eukaryotes, development and organogenesis are often associated with histone modifications. Histone modifications are explained in changes of chromatin composition caused by histone modifying enzymes to covalently alter histone marks, such as acetyl- or methyl group at amino-acids within histone proteins (Agger et al., 2008). Histone modifying enzymes have significant roles in transcriptional regulation by controlling patterns of tissue- and/ or stage-specific gene expression during normal development and organogenesis. Specific histone lysine methylation marks, built by histone methyltransferases (HMTs) and histone demethylases (HDMs), are commonly associated with either the active or the repressive chromatin state; histone H3K4, K36, and K79 methylation and histone acetylation are generally considered as conserved transcriptional active marks, on the other hand, H3K9, K27, and H4K20 methylation as transcriptional repressive marks. Furthermore, the histone marks could be recognition and binding sites of other proteins responsible for various biological processes, such as DNA replication and repair (Kouzarides, 2007).

While histone acetylation is a reversible process regulated by histone acetyltransferases (HATs) and histone deacetyltransferses (HDACs), it was thought that histone methylation was relatively static and could be eliminated through DNA replication or histone exchange (Kooistra & Helin, 2012), before the paper demonstrating the first histone demethylase lysine-specific demethylase 1 (LSD1) that demethylates mono- / dimethyl H3K4 with flavin adenine dinucleotude (FAD)-dependent amine-

oxidation reaction (Shi et al., 2004). It was also revealed that jmjC domain-containing histone demethylase 1 (JHDM1) specifically demethylates H3K36, demonstrating that JmjC domain-containing protein could act as histone lysine emethylase through an oxidative reaction that requires iron Fe(II) and α-ketoglutarate (αKG) as cofactors (Tsukada et al., 2006). After the finding JmjC demethylase family, considerable researches about that have provided the significance of JmjC demethylase in cell development, diseases, and organogenesis from human to plant. This is exemplified by human JMJD3, which is associated with various cancer including lung and liver carcinomas and several haematological malignancies (Agger et al., 2009; Kooistra & Helin, 2012), as well as Arabidopsis relative early flowering 6 (REF6) and rice JMJ706 are required for proper development and organogenesis (Lu et al., 2011; Sun & Zhou, 2008).

JmjC demethylases are commonly classified seven groups according to their protein sequence homology and contained additional domains, and JARID1 subgroup, belonging to JARID group that is one of the seven groups, contains JmjN, BRIGHT/ARID (AT-rich interactive domain, one of the features of JARID group), C5HC2-zinc-finger and PHD domains (Klose et al., 2006). In mammalian, four orthologues contained to human JARID1 subgroup, JARID1A/RBP2, JARID1B/PLU-1, JARID1C/SMCX and JARID1/SMCY, are associated with several cancer types and neurological disorders (Kooistra & Helin, 2012), and it was claimed that Little imaginal discs (LID), the sole JARID group protein in Drosophila, may be an important component of development as a histone lysine demethylase, as well as viability (Li et al., 2007). In budding and fission yeast, Jhd2 (Yjr119c) and Jmj2 (Spac1002.05c) were founded as JARID demethylase

orthologue, respectively, in addition, all of the previously well-studied enzymes in JARID group have been shown that they have the same specific substrates, di- / trimethyl histone H3K4 (Eissenberg et al., 2007; Huarte et al., 2007; Kooistra & Helin, 2012; Seward et al., 2007). Unlike other organisms, functional analysis of JmjC demethylases, especially JARID group, rarely has been conducted in filamentous fungi, especially as plant fungal pathogens.

*Magnaporthe oryzae*, a filamentous fungus, is considered as a destructive fungal pathogens causing rice blast disease (Dean et al., 2012), and the host, rice, is one of the main calorie sources taken by approximately one-half of the world's population (Khush, 2005). Because of the economically significant effect of rice blast disease, *M. oryzae* has been taken the interest of plant pathologists and studied more than 100 years (Leung et al., 1988; Silue et al., 1992) for controls and increasing rice yields. In the early stage of infection, *M. oryzae* elaborates a specialized infection structure, appressoria (Howard & Valent, 1996), which is essential for penetrating host plant cell and could be an effective target of fungicides, such as tricydazole, that inhibit appropriate formation of appressorium (Woloshuk et al., 1983). Thus, considerable knowledge about cAMP, $Ca^{2+}$, and MAP kinase signaling pathways related in appressorium development (Choi et al., 2011; Lee & dean, 1993; Reyna, 2006,; Xu & Hamer, 1996) and pathogenicity related genes (Jeon et al., 2007), has been historically clarified so far, by a lot of genetic researches in *M. oryzae* as a model system for molecular plant-microbe interaction.

In filamentous fungi, epigenetic studies have been emerging recently in histone modifying enzymes, HATs, HDACs, and HMTs (Smith et al., 2011), but researches about HDMs rarely have been done. In *Neurospora crassa* and *Aspergillus nidulans*, histone

acetylation is important roles in transcriptional activation of the genes associated with light response signaling and secondary metabolites (SM) production, respectively (Grimaldi et al., 2006; Shwab et al., 2007). Histone methylation studies in *N. crassa* have revealed that trimethyl H3K9 and DNA metylation are required for heterochromatin formation (Smith et al., 2011; Tamaru, 2001) and methylation of H3K36, regulated by SET-2 methyltransferase, has important roles in fungal growth and conidiation and female sterility (Adhvaryu et al., 2005). In *Aspergillus*, histone methylations are related with SM production, for instance, CclA, a member of COMPASS complex involved in H3K4 methylation, and LaeA, affecting methylation level at H3K9, have a function in regulating SM gene clusters (Bok et al., 2009; Strauss & Reyes-Dominguez, 2011). Recently, in *M. oryzae*, it was showed that MoSET1, catalyzing dimethyl H3K4, is associated with substrate-induced transcriptional activation of a cellulose gene (Vu et al., 2013). It has been defined that histone modification is involved in various biological processes in filamentous fungi, nevertheless the research about fungal histone demethylases needs to be further studied in depth.

In this study, I tried to find what are role of JmjC histone lysine demethylases for fungal development and pathogenicity by functional analysis. First, computational analysis was performed for identifying putative genes encoding JmjC demethylases in *M. oryzae*. Then, deletion mutant of *MoJMJ1* (MGG_04878) belonging to the putative genes was generated, and developmental phenotypes and pathogenicity of the mutant were observed. The deletion of *MoJMJ1* resulted in developmental defects, loss of pathogenicity, and significant changes in transcription of the genes associated with fungal development and pathogenicity. By revealing the function of the putative JmjC

demethylase in fungal development and pathogenicity, this study would provide the epigenetically basic insight into fungal development and control strategies for *M. oryzae* and other closely related plant fungal pathogen species.

# MATERIALS AND METHODS

## I. Fungal strains and culture condition

*Magnaporthe oryzae* wild-type strain KJ201 used in this study was obtained from the Center for Fungal Generic Resources (CFGR, hrtp://genebank.snu.ac.kr). All strains including wild-type strain and mutants generated throughout this study were incubated on V8 juice agar media (8% V8 juice (w/v), 1.5% agar powder (w/v), 10N NaOH) or oatmeal agar media (OMA, 5% oat meal (w/v), 2.5% agar powder (w/v)) at 25℃ under the constant fluorescent light. Mycelia used for RNA, DNA, and protein extraction were incubated in liquid complete media (LCM, 0.6 % yeast extract (w/v), 0.6 % casamino acid (w/v) and 1 % sucrose (w/v)) at 25℃ with 150 rpm shaking. Selection of hygromycin-resistant transformants were carried out using TB3 agar plates (0.3 % yeast extract (w/v), 0.3 % casamino acid (w/v), 1 % glucose (w/v), 20 % sucrose (w/v) and 0.8 % agar powder (w/v)) supplemented with 200 ppm hygromycin B.

## II. Sequence and phylogeneitc analysis

Nucleotide and protein sequences were taken and analyzed at Comparative Fungal Genetic Platform (CFGP, http://cfgp.snu.ac.kr) and NCBI. Sequences of JmjC domain-containing protein were obtained from ChromDB database (www.chromdb.org). Analyze using HMM (Hidden Markov Model) profiling (http://hmmer.janelia.org/) was performed to search additional JmjC proteins in *M. oryzae* and compare the protein sequence homology in an aspect of demethylase function with other organisms. Alignment of

protein sequences was conducted with Clustal W algorithm and T-coffee algorithm. Phylogenetic tree was generated by within MEGA 5.2 using neighbor-joining method with a Poisson correction model and a bootstrap of 1000 replicates. Information about domain architectures was obtained from InterProScan.

## III. Nucleic acid isolation and manipulation

Fungal genomic DNA was extracted by two different methods in according to the purpose. For large-scale screening of transformants, fungal DNA was extracted from mycelia on TB3 agar plates using quick and convenient method (Chi *et al.*, 2009). Genomic DNA extracted by method of using phenol-chloroform was used to Southern blot analysis. Total RNA was extracted by using the Easy-SpinTM total RNA extraction kit (iNtRON Biotechnology, Seoul, Korea) according to the manufacturer's instruction. cDNA for expression analysis by quantitative real-time PCR (qRT-PCR) was synthesized by using ImProm-IITM Reverse Transcription System kit (Promega, Madison, WI, USA) following the manufacturer's instruction.

## IV. Targeted deletion of *MoJMJ1* mutants and complemented strains

To generate gene deletion mutant, homologous recombination strategy was used. The original sequence of MGG_04878.8 was replaced with knock-out construct containing 1.4 kb of hygromycin B phosphotransferase (*HPH*) cassette fused with ~1.2 kb 5'- and 3'- flanking regions by double joint PCR. Protoplast generation and fungal

transformation were performed through PEG mediated transformation. Transformants resistant to hygromycin B within TB3 media were selected. Disruption of genes was verified by PCR using primers for screening (Table 1). Southern blot analysis using genomic DNA was performed to confirm correct integration of *HPH* cassette. Genomic DNA fragments, digested with restriction enzyme, were separated by agarose gel electrophoresis and transferred to nitrocellulose membrane, Hybond-N+ (GE healthcare, NJ, USA). The blot was hybridized with probe labled with $P^{32}$ by using Rediprime™ II Random Prime Labeling System kit (Amersham Pharmacia Biotech, NJ, USA) and the hybridized membrane blot was exposed to imaging plate, BAS-2040 (Fuji Photo Film, Tokyo, Japan) and read by phosphorimage analyzer, BAS-1000 (Fuji Photo Film). Complemented mutant for *MoJMJ1* was generated by similar procedures. DNA fragment containing ORF sequence was amplified from KJ201 genomic DNA. The ORF fragment and pII99 plasmid containing geneticin-resistant gene as a selection marker were co-transformed into protoplast of deletion mutant Δ*Mojmj1*. Complemented mutants were selected on geneticin-supplemented media and selected by PCR and phenotypic assay.

## V. Developmental phenotype assays – Mycelial growth, conidiation, conidial germination, and appressorium formation

Mycelial growth was quantified at 9-day-old by measuring diameter of fungal colonies after incubated in on modified complete agar media modified complete media (1% glucose (w/v), 0.2% peptone (w/v), 0.1% yeast extract (w/v), 0.1% casamino acid (w/v), 0.1% trace element (v/v), 0.6% sodium nitrate (w/v), 0.05% potassium chloride (w/v),

0.05% magnesium sulfate (w/v), 0.15% potassium dihydrogen phosphate (w/v), 1.5% agar powder (w/v)) and 4 mm diameter inoculums were taken from 5-day-old minimal agar media in marginal region.

Conidiation was measured by counting the number of asexual spores in 10 μl of conidia suspension on a haemacytometer. To collect conidia, conidia on 7-day-old V8 juice agar media were rubbed by sterilized cotton swaps with 5 ml sterilized distilled water. Conidiophores development was observed on scrapped 15-day-old oatmeal agar media blocks (1 cm x 1 cm) and captured after 24 hours incubation in moist-lasted airtight containers at room temperature.

For measuring the rates of conidial germination and appressorium formation, conidia were harvested from 7-day-old V8 juice agar media with sterilized distilled water and filtered with two-layers of miracloth (Calbiochem, California, USA). 30 μl of conidial suspensions ($3x10^4$conidia / ml) was dropped on hydrophobic coverslips (W. Knittel Glass, Braunschweig, Germany) with three repeats. The droplets were incubated in moist-lasted airtight containers at room temperature. Incubation time was 12 and eight hours for measuring conidial germination and appressorium formation rates and observing appressorium development, respectively.

## VI. Pathogenicity test, wound inoculation, and sheath assay

For these experiments, conidia on 7-day-old V8 juice agar media were rubbed by sterilized cotton swaps with sterilized distilled water containing tween 20 (250 ppm) and filtered with two-layers of autoclaved miracloth. In preparing conidia for sheath assay, collecting manner was the same, except tween 20 was not contained. Final concentration

of spore suspensions was 5x104 (conidia / ml) for pathogenicity test and wound inoculation, and 2x104 (conidia / ml) for sheath assay. Rice seedlings used for these tests were Oryza satova cv. Nakdongbyeo and 3 or 4-week-old.

For pathogenicity test, spore suspensions (10 ml of total volume) were sprayed to 3-week-old rice seedlings and placed in a dark, humid dew chamber for 18 hours at 25 ℃. They were transferred to a growth chamber in condition 80 % humidity and 25 ℃. Leaves of the rice seedling were collected at 7day after the inoculation and scanned.

Leaves of Nakdongbyeo were used for wound inoculation. Conidial suspensions (5x104 conidia / ml) were dropped at wounds which were picked about 10 times by tip of a sterilized pin. Inoculated leaves were incubated in a humid container at 25 ℃. Lesions were observed and scanned at 6 dpi.

Sheathes of Nakdongbyeo in 5~6 leaf stage were used for rice sheath assay. Rice sheathes were inoculated with conidial suspension (3x104 conidia / ml) and incubated in moist container at 25 ℃. The sheath samples were sliced by razor blade and observed with light microscope.

## VII. Quantitative real-time PCR (qRT-PCR)

qRT-PCR reactions were performed in 10 μl solution that containing 2 μl of cDNA template (12.5 ng / μl), 3 μl of primers (forward and reverse, each primers are 5 pmol) and 5 μl of SYBR® green PCR Master Mix (Applied Biosystems, Warrington, UK). Samples were run by 40 cycles of 15 s at 94 ℃ and 1 min at 60 ℃ after 10 m of denaturation at 94 ℃ on AB7500 Real-Time PCR system (Applied Biosystems).

Threshould of 0.1 was normalized to obtain the threshould cycle (Ct) value from amplification curves. Relative abundance of transcript of target genes was normalized as follows: $2^{-\Delta\Delta Ct}$, where $-\Delta\Delta Ct = (C_{t,\ \text{target gene}} - C_{t,\ \beta\text{-tubulin}}) - (C_{t,\ \text{Wild-type}} - C_{t,\ \beta\text{-tubulin}})$

## VIII. Western blotting analysis

Frozen fungal mycelia were homogenized by homogenizer and added to PRO-PREP™ protein extraction solution (iNtRON Biotechnology, Seoul, Korea). The homogenates were centrifuged (13000 rpm, 10 min, 4 ℃) and the supernatants were collected. Equal amounts of homogenized protein (15 μg) were applied to 12 % SDS-PAGE gel (BIO-RAD, California, USA), and electroblotted onto a Immunobilon-P PVDF membrane (BIO-RAD). For the gel running and transfer procedures, ReliaBLOT® Running Buffer (20X) and Transfer buffer (10X) (BETHYL, Montgomery, USA) were used, respectively. The blots were probed with polyclonal histone H3 and H3K4me3 antibody (Active Motif, California, USA), using Pierce® Fast Western Blot Kit, ECL Substrate (BIO-RAD)

**Table 1. List of oligonucleotide sequences used in this study**

| Name | Sequence (5' → 3') |
|---|---|
| **5'_UF** | GCAAGGACATTGATTACGCG |
| **5'_UF_2.1kb comple.** | GTGACCGTACCATCCAGTTG |
| **5'_UR** | CCTCCACTAGCTCCAGCCAAGCCCGATGGCGAGATGCGGAA |
| **3'_DF** | GTTGGTGTCGATGTCAGCTCCGGAGGGGAGGTAACGGAGGATAC |
| **3'_DR** | ACCGTCAGGGTCGTCCTG |
| **ORF_F_screening** | CGCACAACGAGTTTTGGA |
| **ORF_R_screening** | CGTAGATAGAACCTCTGCG |
| **nested F** | GACTAGATACATGCCAGGG |
| **nested R** | TTCCACATCCTGCGCCA |
| **HYG_F1** | GGCTTGGCTGGAGCTAGTGGAGG |
| **HYG_R1** | CTCCGGAGCTGACATCGACACCAAC |

| Gene | Locus number | Forward (5' → 3') | Reverse (5' → 3') |
|---|---|---|---|
| ***B-tubulin*** | MGG_00604.6 | ACAACTTCGTCTTCGGTCAG | GTGATCTGGAAACCCTGGAG |
| ***CPKA*** | MGG_06368.6 | TCCCAAACCCAGTAGCAAAG | AGTCGGTGATTTTGAGGTGG |
| ***MoPLC1*** | MGG_02444.6 | GAGCTACTCCAAGGAACCAAG | CTCTTGTCCCAGGTGATCTTG |
| ***MAGB*** | MGG_00365.6 | GACTACATGCCTAACGACCAG | GAACATTCGGTAGGTGAGGTC |
| ***MCK1*** | MGG_00883.7 | GGTTTTATGCCGGATTTGAGC | TCTGTGGGAGCATTTGACTG |
| ***MAC1*** | MGG_09898.6 | GCTTTCTGGTCAACTTCATGG | AGGTGTCTAATGCTGAGTGTG |
| ***MoAPS1*** | MGG_09869.6 | AGCTGGTGCTAGTCCCTTCA | CCACCGTTAAATGTCTGGCT |
| ***MoAPS2*** | MGG_08463.6 | CGGCACGGGCGAGAAGA | TTTACCATGCCATCCGACACCT |
| ***MoHOX7*** | MGG_01730.6 | CTGATGTCGGGCATGCAGC | GCTGACTTGGACTCTGCACCAG |
| ***MoCOD2*** | MGG_09263.6 | CCTATACGGGCCCAAGTCTGAA | AACATTATTTGCCGGCCCGT |
| ***MoJMJ1*** | MGG_04878.7 | ACGGTAAATGTCTCAAGGTGG | AAAGTAGGTCTTCAAGGTTCGG |
| ***MGG_04877*** | MGG_04877.7 | CAAAGTGCCGAGGGATATGAG | CCTTGGGTATCAGCTCTTGTG |

# RESULTS

## I. Identification of putative genes encoding JmjC histone demethylase in *M. oryzae*

First of all, putative genes encoding JmjC domain-containing proteins (IPR003347) in *M. oryzae* were identified by InterProScan, and eleven of JmjC domain-containing protein was searched in *M.oryzae*. To predict functionally active JmjC histone demethylase genes in M. oryzae, Hidden-Markov profiling was conducted. As a result, a total of seven putative JmjC demethylase genes were predicted to have demethylase activity in practice (Table 2). Secondly, a phylogenetic tree was prepared to figure out which JmjC group the genes are classified in. As human JmjC demethylases were well-studied, classification of human JmjC demethylase group was referred. JmjC protein sequences of human, rice, *Arabidopsis* and yeast were used for phylogenetic analysis. Among the predicted seven genes in *M. oryzae*, one gene (MGG_04878) was predicted to belong to JARID group, and other two genes (MGG_09186 and MGG_01068) were contained to JMJD2 and JHDM2, respectively. Other two (MGG_01543 and MGG_04401) belonged to JmjC domain only groups, and the others (MGG_09841 and MGG_02045) appeared to be fungal specific through phylogenetic analysis (Fig. 1). Finally, MGG_04878, belonging to JARID group, was selected for functional characterization, and named *M. oryzae jumonji 1* (*MoJMJ1*).

**Table 2. The list of genes encoding putative JmjC demethylase in *M. oryzae***

| Gene name | Locus | Size of gene (nt) | Size of protein (aa) |
|---|---|---|---|
| ***MoJMJ1*** | MGG_04878.7 | 5,933 | 1,756 |
| ***MoJMJ2*** | MGG_09841.7 | 1,260 | 420 |
| ***MoJMJ3*** | MGG_09186.7 | 4,739 / 5,082 | 1,504 / 1,530 |
| ***MoJMJ4*** | MGG_01543.7 | 1,599 | 532 |
| ***MoJMJ5*** | MGG_04401.7 | 1,631 | 506 |
| ***MoJMJ6*** | MGG_01068.7 | 4,038 | 1,345 |
| ***MoJMJ7*** | MGG_02045.7 | 3,415 | 1,104 |

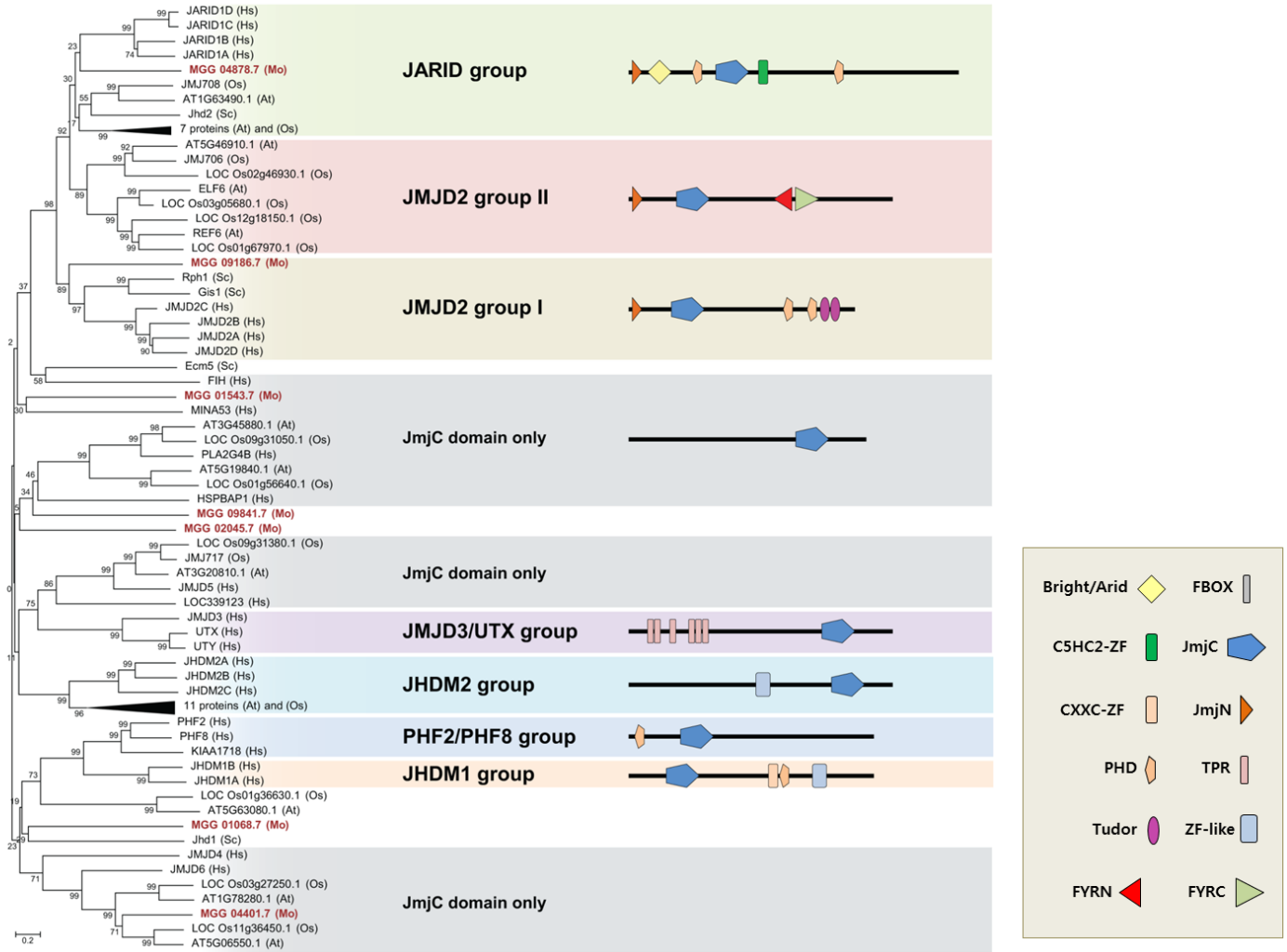
JARID1D (Hs)
JARID1C (Hs)
JARID1B (Hs)
JARID1A (Hs)
MGG 04878.7 (Mo)
JMJ708 (Os)
AT1G63490.1 (At)
Jhd2 (Sc)
7 proteins (At) and (Os)
AT5G46910.1 (At)
JMJ706 (Os)
LOC Os02g46930.1 (Os)
ELF6 (At)
LOC Os03g05680.1 (Os)
LOC Os12g18150.1 (Os)
REF6 (At)
LOC Os01g67970.1 (Os)
MGG 09186.7 (Mo)
Rph1 (Sc)
Gis1 (Sc)
JMJD2C (Hs)
JMJD2B (Hs)
JMJD2A (Hs)
JMJD2D (Hs)
Ecm5 (Sc)
FIH (Hs)
MGG 01543.7 (Mo)
MINA53 (Hs)
AT3G45880.1 (At)
LOC Os09g31050.1 (Os)
PLA2G4B (Hs)
AT5G19840.1 (At)
LOC Os01g56640.1 (Os)
HSPBAP1 (Hs)
MGG 09841.7 (Mo)
MGG 02045.7 (Mo)
LOC Os09g31380.1 (Os)
JMJ717 (Os)
AT3G20810.1 (At)
JMJD5 (Hs)
LOC339123 (Hs)
JMJD3 (Hs)
UTX (Hs)
UTY (Hs)
JHDM2A (Hs)
JHDM2B (Hs)
JHDM2C (Hs)
11 proteins (At) and (Os)
PHF2 (Hs)
PHF8 (Hs)
KIAA1718 (Hs)
JHDM1B (Hs)
JHDM1A (Hs)
LOC Os01g36630.1 (Os)
AT5G63080.1 (At)
MGG 01068.7 (Mo)
Jhd1 (Sc)
JMJD4 (Hs)
JMJD6 (Hs)
LOC Os03g27250.1 (Os)
AT1G78280.1 (At)
MGG 04401.7 (Mo)
LOC Os11g36450.1 (Os)
AT5G06550.1 (At)
0.2
JARID group
JMJD2 group II
JMJD2 group I
JmjC domain only
JmjC domain only
JMJD3/UTX group
JHDM2 group
PHF2/PHF8 group
JHDM1 group
JmjC domain only
Bright/Arid
FBOX
C5HC2-ZF
JmjC
CXXC-ZF
JmjN
PHD
TPR
Tudor
ZF-like
FYRN
FYRC

**Figure 1. Comparative analysis of MoJMJ1 with other organisms**

Phylogenetic analysis of MoJMJ protein sequences. JmjC demethylase protein sequences of human, *Arabidopsis*, rice and yeast were taken from . Alignment was conducted by using ClusterW algorithm within MEGA 5.2 program, and phylogenetic tree was generated by neighbor-joining method. Abbreviation for species: Hs, *Homo sapiens*; At, *Arabidopsis thaliana*; Os, *Oryza sativa*; Sc, *Saccharomyces cerevisiae*; Mo, *Magnaporthe oryzae*

## II. Domain architecture and conserved motifs in JmjC domain of MoJMJ1

In JARID1 group, several orthologues have been characterized from human, Drodophila, *C. elegans* to yeast and *S. pombe*. The majority of the JARID1 group proteins have been reported to have the same target histone residues, di- and trimethyl H3K4, and they contain highly conserved cofactor binding sites, which are compatible with their enzymatic activity (Agger et al., 2008; Liang et al., 2007; Huarte et al., 2007; Klose et al., 2006; Secombe et al., 2007). To predict the potential that MoJMJ1 is an active enzyme, domain architecture and cofactor binding residues within JmjC domain were compared with other proteins within JARID1 group. MoJMJ1 protein contains JmjN (IPR003349), JmjC (IPR003347), BRIGHT/ARID (IPR001606), C5HC2-zf (IPR004198), and PHD domain, and the composition looks very similar with human JARID1 orthologues (Fig. 2A). Multiple sequence alignment shows that MoJMJ1 also has highly conserved cofactor binding residues (Fig. 2B), which are composed of Fe(II)-/αKG-binding sites and crucial for enzymatic activity and substrate specificity. These predictions provide the evidence that JmjC domain in MoJMJ1 could actively catalize di-/ trimethyl H3K4.

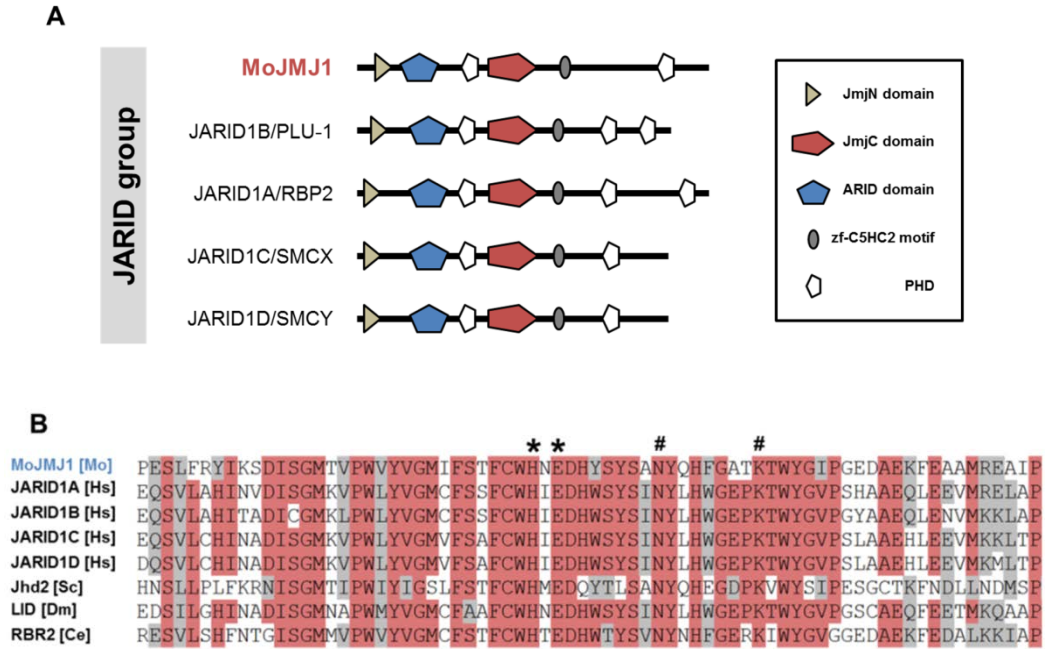


**Figure 2. Domain architectures and conserved key amino acids for demethylase activity in JmjC domain**

(A) Schematic representation of domains in MoJMJ1. Domain architecture was obtained from InterProScan.

(B) Protein sequence alignment of JmjC domains in other organisms including MoJMJ1. Proteins of other organisms were previously studied and revealed that have histone lysine demethylase activity. Asterisk (*) and number sign (#) mean Fe(II) and α-ketoglutarate binding site, respectively. Abbreviation for species: Hs, *Homo sapiens*; Sc, *Saccharomyces cerevisiae;* Dm, *Drosophila melanogaster*; Ce, *Caenorhabditis elegans*

## III. Targeted gene disruption of *MoJMJ1*

To reveal the functions of JARID group demethylase in fungal development and pathogenicity, targeted gene deletion mutant was generated via homologous recombination. Original *MoJMJ1* sequence in wild-type strain, KJ201, was replaced with manipulated construct containing *HPH* cassette (Fig. 3A). Correct gene integration was checked through PCR screening by using ORF primers (Table 1). Genomic DNA of wild-type and Δ*Mojmj1* mutants were digested by *Sal*I for hybridization with probe, 5' flanking region, and Southern blot analysis was conducted (Fig. 3B), determining that single copy of *HPH* cassette was inserted into correct location. It was also confirmed that transcript of *MoJMJ1* is not expressed in both of Δ*Mojmj1* mutant strain (Fig. 3C).

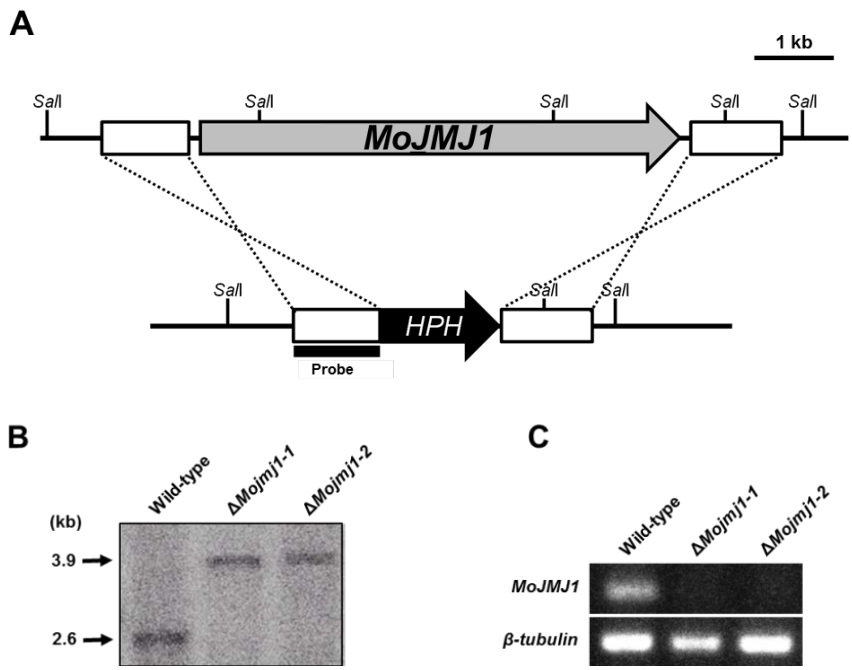


**Figure 3. Targeted gene replacement of *MoJMJ1* in *M. oryzae***

(A) Schematic representation for *MoJMJ1* targeted gene deletion. DNA construct was made by fusion PCR. *MoJMJ1* was replaced with *HPH* cassette by homologous recombination.

(B) Southern blot analysis performed to confirm insertion of single copy DNA construct. Genomic DNA was digested with *SalI* and probed with 5' flanking fragment of *MoJMJ1*.

(C) Reverse transcriptase PCR for expression of *MoJMJ1*. RNA were extracted from mycelia of wild-type (lane 1), Δ*Mojmj1-1* (lane 2), Δ*Mojmj1-2* (lane 3) and *MoJMJ1c* (lane 4). cDNA synthesis was done using reverse transcriptase and PCR performed with qRT-PCR primers (Table. 4) using the cDNA templates.

## IV. Vegetative growth of Δ*Mojmj1* mutants

Phenotypes of Δ*Mojmj1* were investigated to clarify the functions of *MoJMJ1* in vegetative and developmental stages. First, mycelial growth was observed in order to test effect of *MoJMJ1* on fungal vegetative stage. The diameter of ΔMojmj1 mutants showed reduction of 20 % in comparison with wild-type at 9 dpi on complete agar media (Fig. 4B). In addition, autolysis was observed in both deletion mutants (Fig. 4A). Complement strain of *MoJMJ1*, *MoJMJ1c*, restored the all defects in the level of wild-type (Fig. 4A and B), indicating that *MoJMJ1* is involved in normal vegetative growth in *M. oryzae*.

Furthermore, vegetative growth of Δ*Mojmj1* mutants showed no difference in minimal agar media, and carbon and nitrogen source starvation media (data not shown). As the results, vegetative growth of Δ*Mojmj1* was not affected by nutrient, suggesting that Δ*Mojmj1* is not auxotroph mutant and function of *MoJMJ1* in vegetative growth is not associated with nutrient.

A

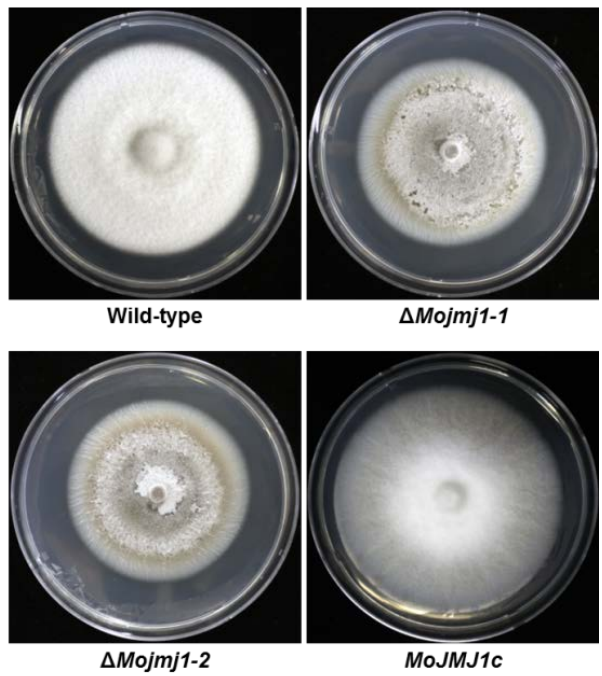
Wild-type
ΔMojmj1-1
ΔMojmj1-2
MoJMJ1c

B

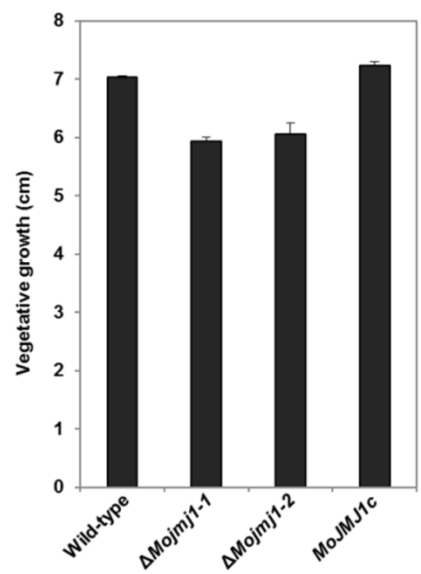
Vegetative growth (cm)
0
1
2
3
4
5
6
7
8
Wild-type
ΔMojmj1-1
ΔMojmj1-2
MoJMJ1c

**Figure 4. Mycelial growth on complete media of Δ*Mojmj1***

(A) Colony morphology of wild-type, Δ*Mojmj1* mutants, and *MoJMJ1c* on complete agar media. Photographs were taken at 9 day after inoculation.

(B) Mycelial growth of wild-type, Δ*Mojmj1* mutants, and *MoJMJ1c*. Radial growth was measured as its diameter at 9-day-old on complete agar media.

## V. Asexual reproduction of Δ*Mojmj1* mutants

The concentration of conidia was counted to reveal whether the asexual reproduction of *M. oryzae* is affected by MoJMJ1. After incubation for 7 days, the concentrations of conidia collected from colony of Δ*Mojmj1* mutants were 25 ~ 40 % of wild-type, and *MoJMJ1c* recovered the defect up to 75 % (Fig. 5A).

Conidia and conidiophores were captured in detail during 24 hours incubation on agar blocks in an effort to investigate reason of the reduction in conidia. Although it appeared that there are no defects in ability to form conidia from conidiophores, the number of conidiophores itself decreased in Δ*Mojmj1* mutants (Fig. 5B). This suggests that *MoJMJ1* is associated with asexual reproduction in an aspect of conidiophores development.

A

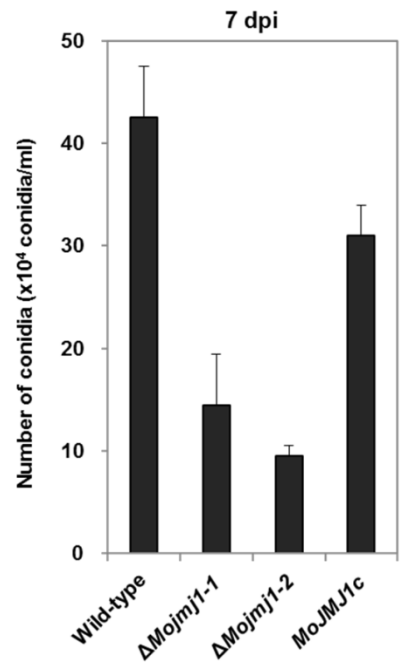
7 dpi
Number of conidia (x10⁴ conidia/ml)
50
40
30
20
10
0
Wild-type
ΔMojmj1-1
ΔMojmj1-2
MoJMJ1c

B

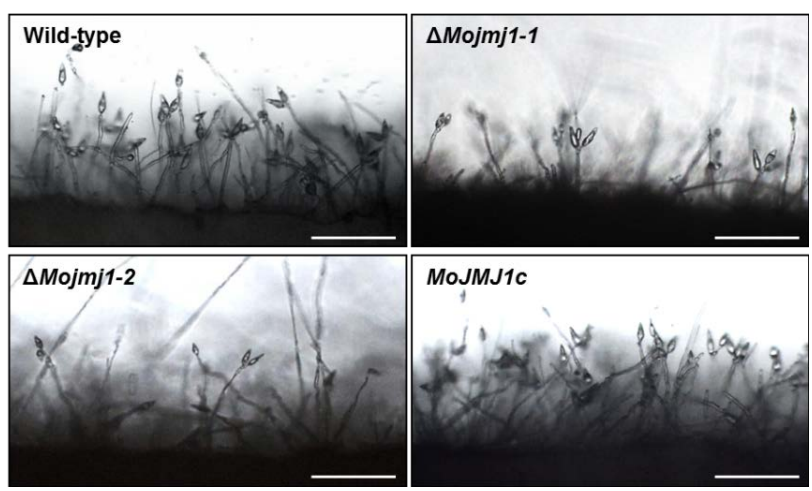
Wild-type
ΔMojmj1-1
ΔMojmj1-2
MoJMJ1c

**Figure 5. Conidiation and conidiophore development of Δ*Mojmj1***

(A) Comparison of the number of conidia ($x10^4$ conidia / ml) produced by wild-type, Δ*Mojmj1* and *MoJMJ1c*. Conidia were collected from 7-day-old V8 agar media.

(B) Light microscopic images of conidia and conidiophores development of wild-type, Δ*Mojmj1* and *MoJMJ1c* on oat-meal agar block were captured after 24 hours incubation. Scale bars = 100 μm

## VI. Conidial germination and appressorium development of Δ *Mojmj1*

Normal development of appressoria is a critical process for *M. oryzae* to penetrate host cells. To clarify whether *MoJMJ1* affects in conidial germination and appressorium formation, conidia were observed on artifact hydrophobic surface. Most of conidia germinated at 12 hours after drop in all strains including deletion mutants (Fig. 6B). While the conidia of Δ*Mojmj1* recorded normal germination rate, they showed bipolar germ-tubes with branches at 8 hours after drop (Fig. 6A). Moreover, more than 95 % of the conidia in Δ*Mojmj1* failed to develop appressoria, and *MoJMJ1c* recovered the all defects in germination and appressorium formation up to the level of wild-type (Fig. 6A and C). Whereas *MoJMJ1* does not affect in conidial germination itself, it is essential for appressorium formation.

The germ-tubes of Δ*Mojmj1* mutants elongated abnormally and appeared to have several rounds of swelling and hooking until 8 hours after drop (Fig. 6A), growing like vegetative hyphae with excessive branches after prolonged incubation. Furthermore, abnormal appressorium appeared at the tip of excessively elongated germ-tubes of Δ*Mojmj1* from 20 hours after drop, and the rate of conidia with abnormal appressoria increased up to 30 ~ 40% at 36 hours after drop on artifact hydrophobic surface (Fig. 7). Taken together, *MoJMJ1* is essential for normal development in germ-tubes and appressorium.

To investigate whether *MoJMJ1* is associated with signaling-pathway for appressorium formation, chemical complementation was performed by treating cAMP,

$CaCl_2$, and 1,16-hexadecanediol (HDD) into conidial suspension of Δ*Mojmj1* on hydrophobic surface at 16 hours after drop. None of the chemicals restored the defect in appressorium formation (data not shown).

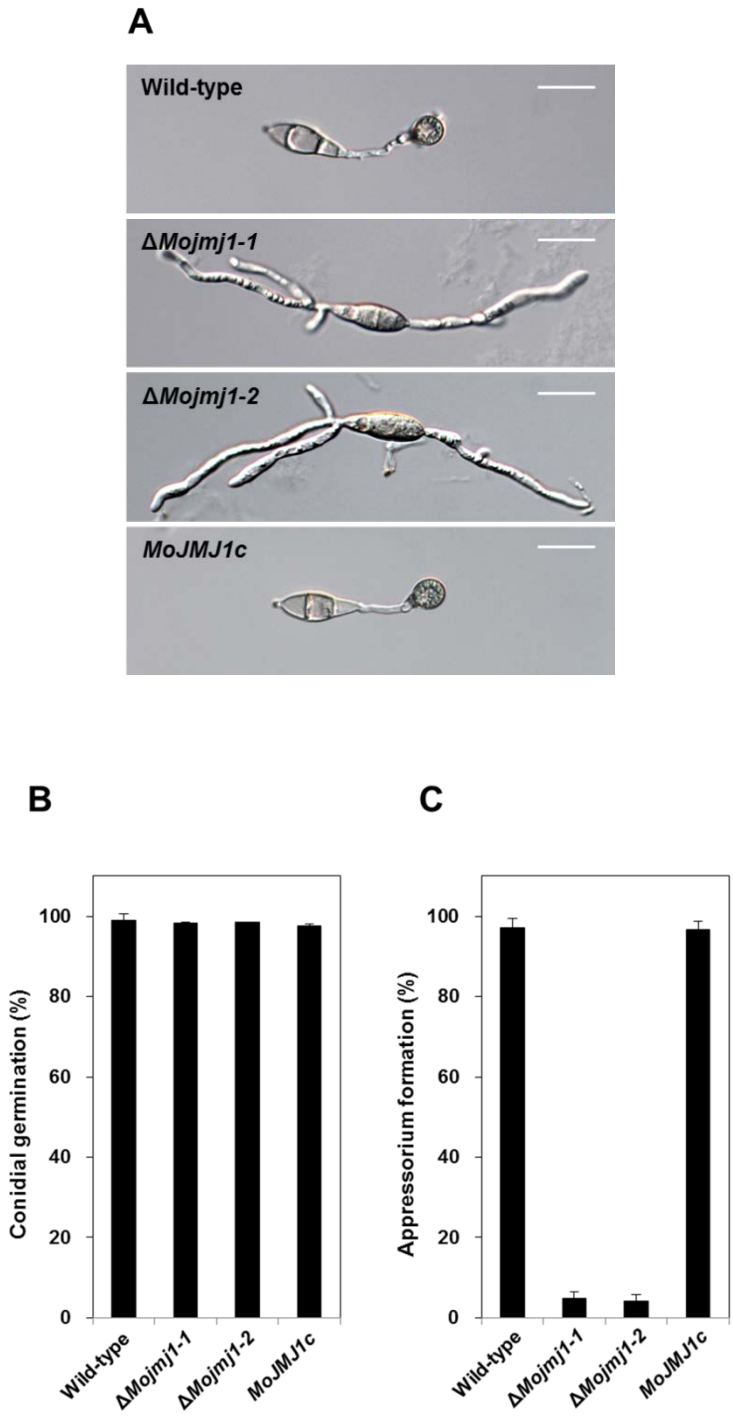
A
Wild-type
ΔMojmj1-1
ΔMojmj1-2
MoJMJ1c
B
Conidial germination (%)
100
80
60
40
20
0
Wild-type
ΔMojmj1-1
ΔMojmj1-2
MoJMJ1c
C
Appressorium formation (%)
100
80
60
40
20
0
Wild-type
ΔMojmj1-1
ΔMojmj1-2
MoJMJ1c

**Figure 6. Conidial germination and appressorium development of Δ*Mojmj1* and *MoJMJ1c***

(A) Appressorium formation of wild-type, Δ*Mojmj1* and *MoJMJ1c* were observed at 8 hours after drop and incubation on hydrophobic coverslips. Conidia were harvested from 7-day-old V8 juice agar media. Scale bars = 20 μm

(B) Conidial germination rates of wild-type, Δ*Mojmj1* and *MoJMJ1c*. Conidia were harvested from 7-day-old V8 juice agar media. Conidia were incubated on hydrophobic coverslips at 12 hours after drop. Rates were measured from at least three experiments with minimum 100 conidia each.

(C) Appressorium formation rates of wild-type, Δ*Mojmj1* and *MoJMJ1c* in the same condition of (B). Rates were measured from at least three experiments with minimum 100 germinated conidia each.

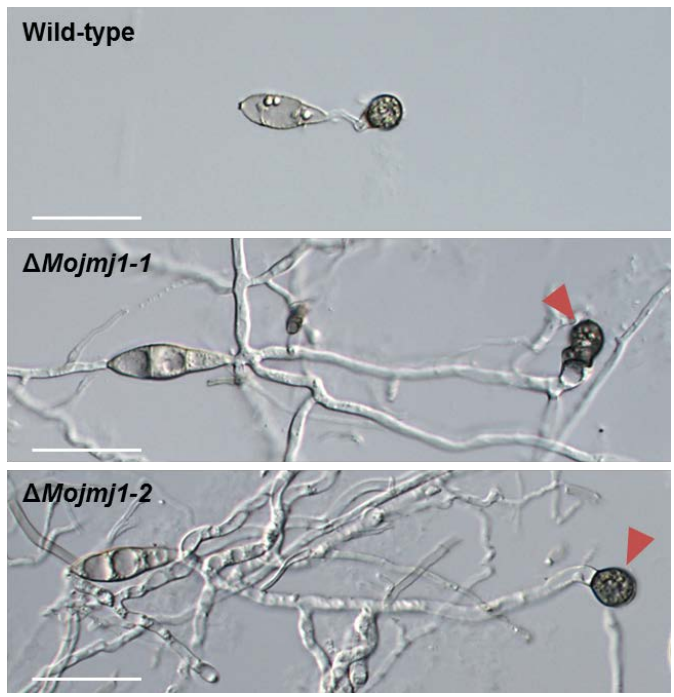


**Figure 7. Abnormal appressorium formation of Δ*Mojmj1***

Abnormal appressorium formation of wild-type and Δ*Mojmj1* mutants captured at 36 hours after drop on hydrophobic coverslips. Arrows indicate appressorium. Scale bars = 30 μm

**Table 3. Four phenotypes of wild-type, Δ*Mojmj1* mutants, and complementation strain *MoJMJ1c***

| Strain | Mycelial growth on CM (cm) | Conidiation ($x10^4$ / ml) | Germination (%) | Appressorium formation (%) |
|---|---|---|---|---|
| **Wild-type** | 7.03 ± 0.03 | 43 ± 5 | 98.91 ± 1.75 | 97.16 ± 2.32 |
| **Δ*Mojmj1-1*** | 5.94 ± 0.06 | 14 ± 5 | 98.19 ± 0.23 | 4.73 ±1.73 |
| **Δ*Mojmj1-2*** | 6.07 ± 0.19 | 9 ± 1 | 98.44 ± 0.20 | 4.04 ±1.73 |
| ***MoJMJ1c*** | 7.24 ± 0.06 | 31 ± 3 | 97.58 ± 1.48 | 96.58 ± 2.22 |

Germination and appressorium formation rates were measured at 12 hours after incubation.

## VII. Host penetration of Δ*Mojmj1* mutants

As Δ*Mojmj1* has defect in appressorium formation on the artifact hydrophobic surface, it was predicted that *MoJMJ1* is indispensable for fungal pathogenesis. To confirm that, pathogenicity test was performed. While the leaves inoculated with wild-type shows severe lesion, those of deletion mutants remain intact at 7 dpi (Fig. 8). Δ*Mojmj1* lost pathogenicity in according to the prediction, which was resulted from irregular appressorium formation. Although the complemented mutant showed restoring normal appressorium formation morphologically, *MoJMJ1c* couldn't show disease symptom (Fig. 8), suggesting that the recovered appressoria could not overcome the defect functionally.

To identify cause of the problem, rice sheath assay was conducted. Although wild-type reached early infection stage, after penetration, showing the typical penetration peg at 24 hpi (Fig. 9A), only normal appressoria was shown without penetration peg in *MoJMJ1c* (Fig. 9G). In order to reveal whether the observation was caused by delay of penetration process or not, it was also performed at 48 hpi. While wild-type conidia was filling one host cell with invasive hyphae and crossing into other cells (Fig. 9B), *MoJMJ1c* was still staying at the surface of rice sheath cells (Fig. 9H). In both of the deletion mutants, abnormal appressorium, which seem like hypha-driven appressorium (Kim et al., 2009), were observed at 24 and 48 hpi (Fig. 9C ~ F), and they completely couldn't penetrate as appressorium on the surface of host cells. The abnormal appressorium on surface of sheath cell were shown within about less than 30 % of the conidia in Δ*Mojmj1* mutants, which was similar with the result on artifact hydrophobic surface of Fig. 7. Given the penetration defects of Δ*Mojmj1*, it is indicated that *MoJMJ1* is required for pathogenesis.

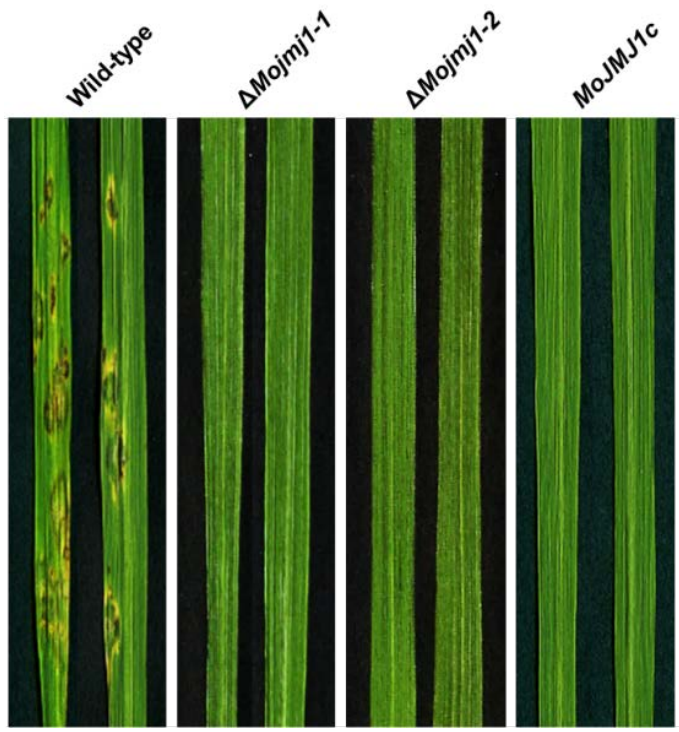


**Figure 8. Pathogenicity of Δ*Mojmj1* and *MoJMJ1c***

Pathogenicity test of Δ*Mojmj1*, *MoJMJ1c* mutants, and *MoJMJ1c* was performed via spray inoculation. Conidial suspensions ($5x10^4$ conidia / ml) were sprayed to 3-week rice seedlings and leaves of the rice seedling were collected at 7day after inoculation.

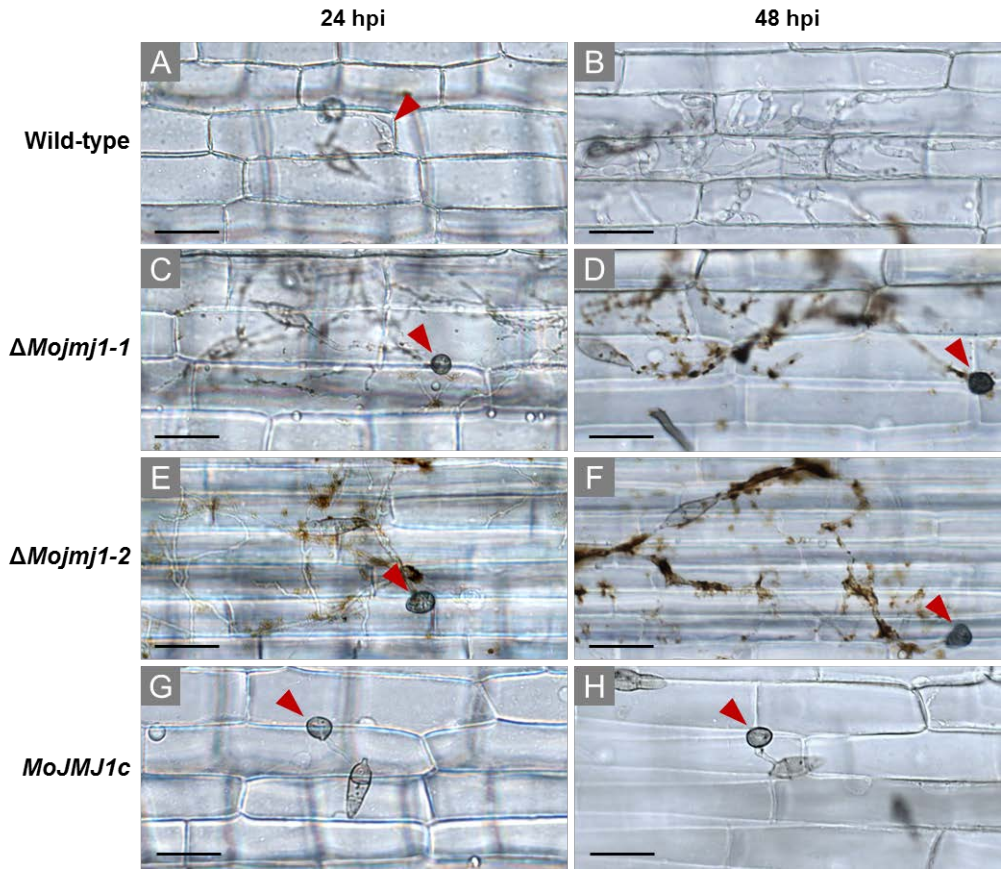


**Figure 9. Rice sheath assay of Δ*Mojmj1* and *MoJMJ1c***

(A) ~ (H) Rice sheath was inoculated with conidial suspension ($2x10^4$ conidia / ml). Arrows indicate appressorium. Scale bars = 30 μm

(A), (C), (E), and (G) Invasive growth was observed at 24 hpi.

(B), (D), (F), and (H) Invasive growth was observed at 48 hpi.

## VIII. Invasive growth of Δ*Mojmj1* mutants

Wound inoculation was conducted to examine whether *MoJMJ1* has an impact on invasive growth within host cells, because interaction between host and pathogen couldn't be monitored in Δ*Mojmj1*, which was resulted from penetration defect. Considering about 20 % of delay in vegetative growth, invasive growth of Δ*Mojmj1* mutants caused relatively severe defects in comparison with wild-type (Fig. 10). *MoJMJ1c* also showed the same result of Δ*Mojmj1* (Fig. 10), it could be thought that *MoJMJ1* is not the only factor bringing about the defect in invasive growth, but associated with the host-pathogen interaction.

ROS from plant cell restricts invasive hyphal growth through its toxicity (Tanabe et al., 2009). To test ROS sensitivity of Δ*Mojmj1*, vegetative growth was observed on media containing 5 mM of $H_2O_2$ at 9 dpi. Vegetative growth of Δ*Mojmj1* on $H_2O_2$ media was not different that on complete agar media (data not shown), indicating that function of MoJMJ1 in invasive growth is possibly independent of plant defense mechanism with ROS.

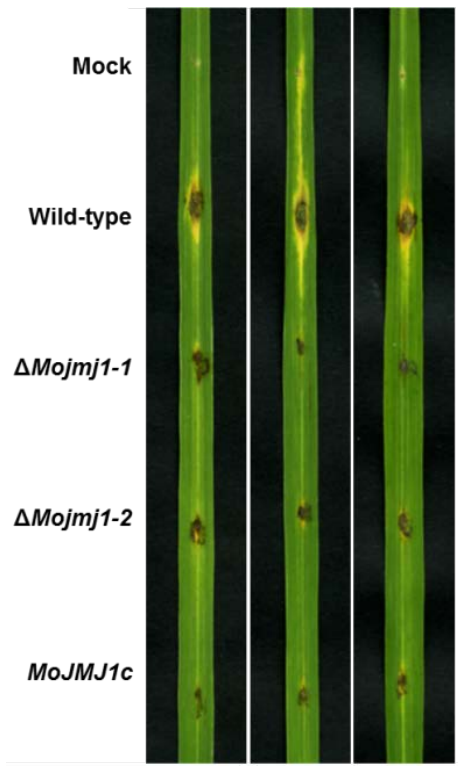


**Figure 10. Invasive growth of Δ*Mojmj1* and *MoJMJ1c* on rice leaves**

Wound inoculation was observed at 5 dpi after drop of conidial suspensions ($5x10^4$ conidia / ml) on wounded spots of rice leaves.

## IX. Transcriptional regulation of the development and pathogenicity-related genes

Quantitative RT-PCR (qRT-PCR) was performed to test expression of fungal development and pathogenicity-related genes associated with phenotypic defects of Δ*Mojmj1* (table 3). Expressions of *MoPLC1*, *MAC1* and *MAGB*, which are involved in signal transduction cascades as upstream regulators, were significantly reduced in Δ*Mojmj1*. This suggests that *MoJMJ1* perhaps regulates $Ca^{2+}$ and cAMP-dependent signaling pathways in appressorium development by affecting genes known as upstream regulators. Reduced expression of *MoHOX7*, which is essential for normal appressorium formation, was especially coincident with the phenotypic defects of Δ*Mojmj1*. The Other *M. oryzae* transcription factor (TF) genes, *MoAPS1*, *MoAPS2* and *MoCOD2*, involved in conidiogenesis also showed significant changes (Fig. 11). Given this expression profile, it is presumed that MoJMJ1 regulates transcription of the genes required for fungal development.

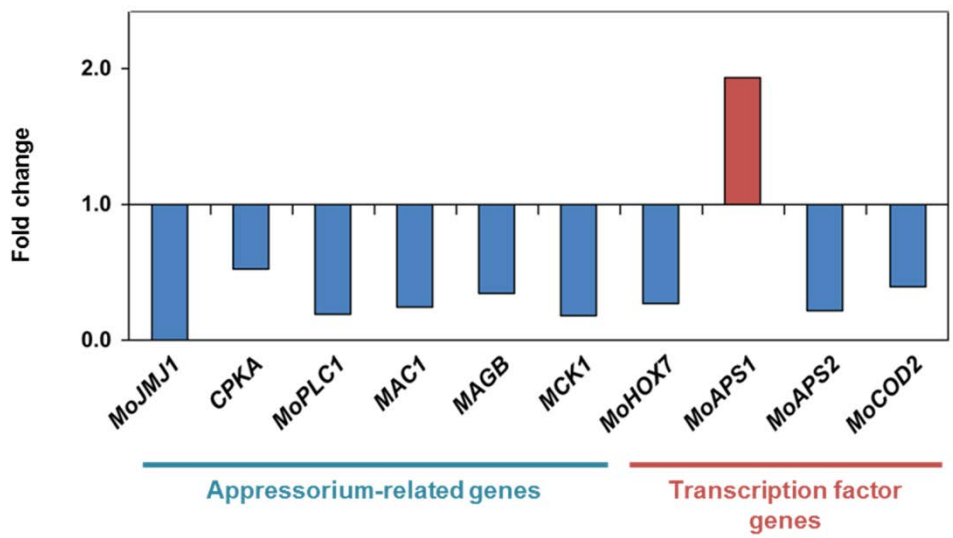


**Figure 11. Expression profiles of development-related genes in Δ*Mojmj1***

Expression of development-related *M. oryzae* genes in mycelial stage of Δ*Mojmj1*. *β-tubulin* gene is reference gene. The color of bars means Blue ≤ 0.5 and red ≥ 2.0.

**Table 4. Phenotypes of the fungal development-related genes used for qRT-PCR**

| | Gene | Phenotypic defect |
|---|---|---|
| Appressorium-related genes | CPKA | Appressorium formation, cAMP responsiveness, pathogenicity |
| | MAC1 | Vegetative growth, conidiation, Appressorium formation, pathogenicity |
| | MoPLC1 | Appressorium formation, pathogenicity |
| | MAGB | Vegetative growth, conidiation, Appressorium formation |
| | MCK1 | Autolysis, cell wall integrity, conidial production, Appressorium development |
| Transcription factor genes | MoHOX7 | Hyphal-driven app. formation |
| | MoAPS1 | Conidial production |
| | MoAPS2 | Conidial production |
| | MoCOD2 | Conidial reproduction, pathogenicity |

## X. Immunoblot assay of MoJMJ1

Trimethyl H3K4 at the 5’ end of genes is well known as a transcriptional active mark (Kooistra & Helin, 2012; Lee et al., 2007), and MoJMJ1 was predicted to remove di- / trimethyl group at H3K4 as a demethylase. Western blot analysis was performed in order to examine that MoJMJ1 has an enzymatic activity, as well as it regulates transcription of target genes through modulation of trimethyl H3K4 levels. The amounts of protein detected by trimethyl H3K4-specific antibody would be increase in Δ*Mojmj1*, if MoJMJ1 affects as a demethylase around global H3K4 methylation levels. However, there was no significant difference in the amounts of detected proteins between wild-type and Δ*Mojmj1* (Fig. 12). According to this result, MoJMJ1 does not affect H3K4 methylation at the level of total protein, but it cannot be excluded that MoJMJ1 would increase trimethyl H3K4 levels at target genes in a relatively few amount of modulation.

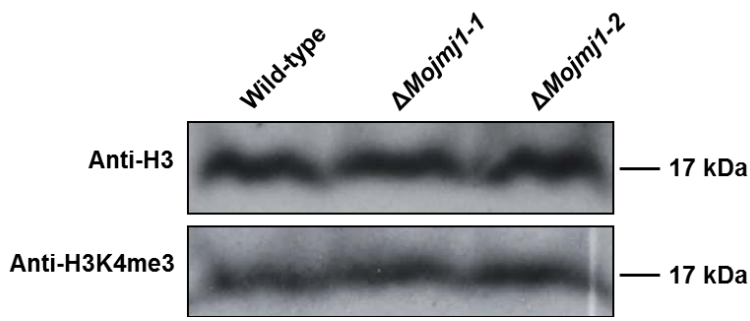


**Figure 12. Western blot analysis for Wild-type and Δ*Mojmj1* proteins**

Proteins were extracted from mycelia of wild-type (lane 1), Δ*Mojmj1-1* (lane 2), Δ*Mojmj1-2* (lane 3). Separated proteins were transformed to from SDS-PAGE gel to nitrocellulose membrane and the blot was probed with polyclonal anti-H3 antibody (upper panel) and polyclonal anti-trimethyl H3K4 antibody (lower panel) as primary antibody.

## XI. Complementation assay of *MoJMJ1*

In the previous experiments, the complemented mutant, *MoJMJ1c*, restored several phenotypic defects in vegetative growth, autolysis, asexual reproduction, conidial germination and appressorium development, but not all. The penetration and invasive growth defects, related with pathogenicity, couldn't be overcome by the native *MoJMJ1* construct with 1.2 kb 5' upstream flanking region (Fig. 13A). To investigate the partial complementation caused by shorter 5' upstream region than that for fully complementation, longer *MoJMJ1* construct was regenerated with 2.1 kb 5' upstream region (Fig. 13B) and transformed to Δ*Mojmj1* protoplast.

Primary phenotypes were observed with the regenerated complements, *MoJMJ1c_4*, *MoJMJ1c_13* and *MoJMJ1c_27*. All the three strains make normal appressorium developed on artifact hydrophobic surface (Fig. 14A), but could not cause disease (Fig. 14B). These results are identical to formers, indicating that reason of the partial complementation is not related with promoter length.

To test other possibility that wild-type protoplast used for Δ*Mojmj1* mutant generation has some problems, such as loss of pathogenesis, ectopic stains (*MoJMJ1e_52* and *MoJMJ1e_185*) were sprayed to rice leaves. In conclusion, it was revealed that wild-type protoplast is not the reason for partial complementation by confirming lesions caused by the ectopic strains (Fig. 14C).

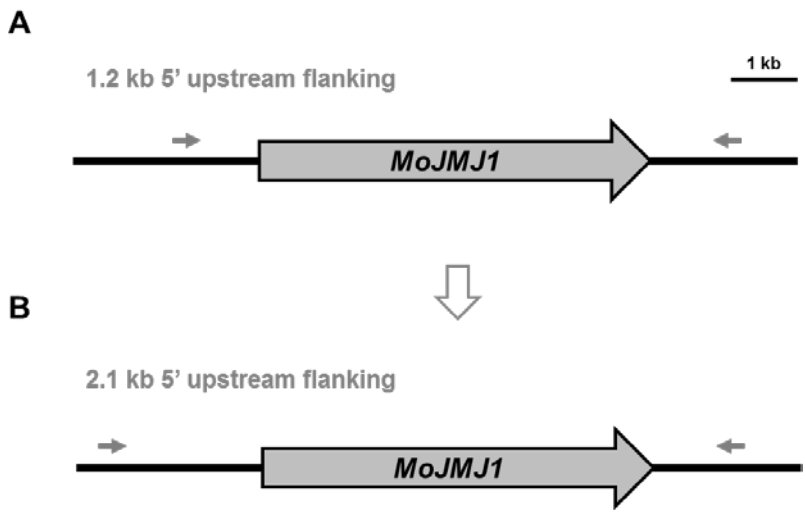


**Figure 13. Regeneration of complement strains**

(A) Schematic representation for complemented mutant *MoJMJ1c*. Two arrows mean the primer binding sites on wild-type genomic DNA for PCR-amplified constructs. The size of 5' upstream flanking region is about 1.25 kb.

(B) Schematic representation for re-generated *MoJMJ1c* whose extended 5' upstream flanking region. Two arrows mean the primer binding sites on wild-type genomic DNA for PCR-amplified constructs. The size of 5' upstream flanking region is about 2.1 kb.

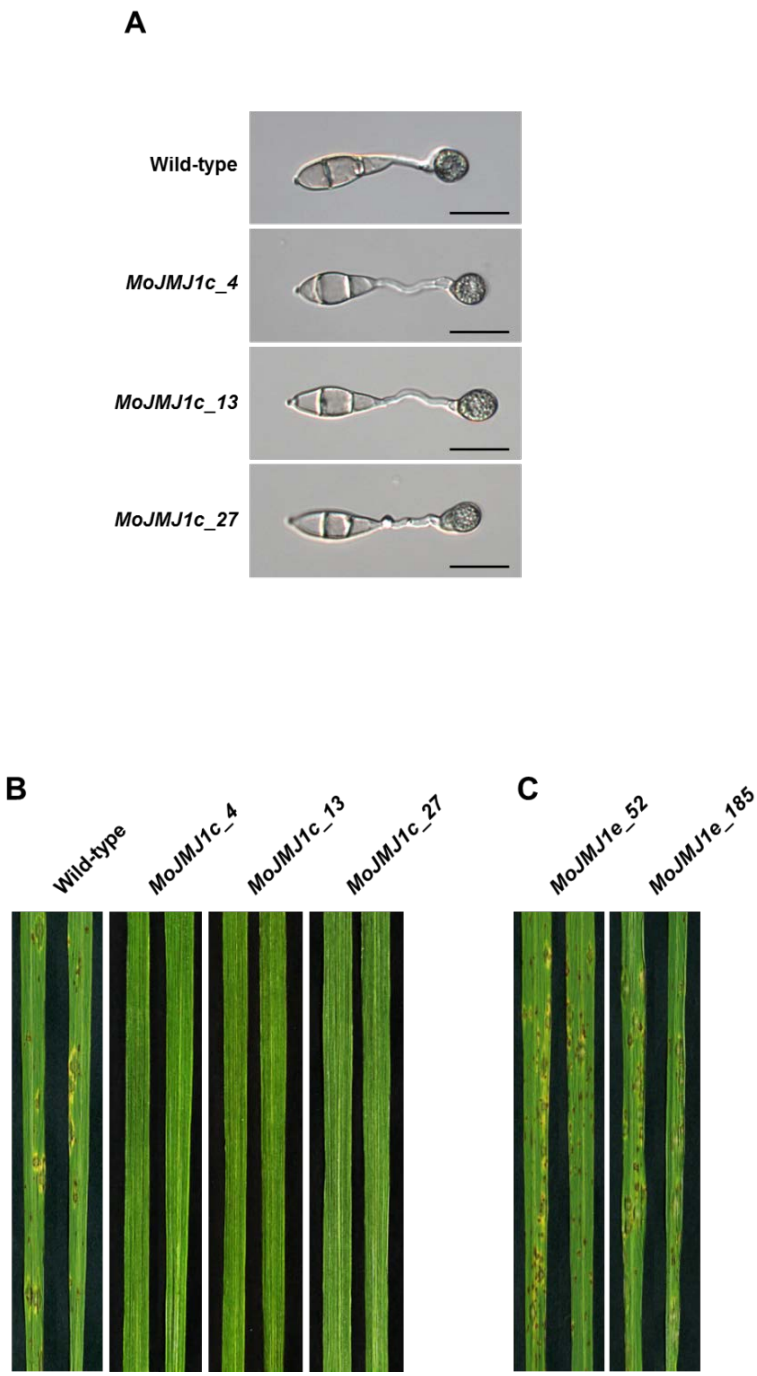
A
Wild-type
MoJMJ1c_4
MoJMJ1c_13
MoJMJ1c_27
B
Wild-type
MoJMJ1c_4
MoJMJ1c_13
MoJMJ1c_27
C
MoJMJ1e_52
MoJMJ1e_185

**Figure 14. Appressorium development and pathogenicity test of regenerated complement strains**

(A) Appressorium formation of wild-type and regenerated complement mutant strains (*MoJMJ1c_4*, *13*, and *27*) transformed with construct of 2.1kb 5' flanking region. Scale bars = 20 μm

(B) Pathogenicity of wild-type and regenerated complement mutant strains (*MoJMJ1c_4*, *13*, and *27*) transformed with construct of 2.1kb 5' flanking region. Pathogenicity test was performed via spray inoculation. Conidial suspensions ($5x10^4$ conidia / ml) were sprayed to 3-week rice seedlings and leaves of the rice seedling were collected at 7day after inoculation.

(C) Pathogenicity test of ectopic strains (*MoJMJ1e_52* and *185*) was performed at the same time with test of (B)

# DISCUSSION

Conidiogenesis and appressorium development are essential steps for fungal pathogen to infect host plant. Knowledge of biological networks in the steps was historically accumulated by many researchers, but not in an aspect of epigenetics, especially histone demethylation. It is well known that histone demethylases are involved in cell development and lots of biological process. To clarify the roles of JmjC histone demethylase for development and pathogenicity in *M. oryzae,* a functional analysis was performed.

There are eleven genes encoding JmjC domain-containing proteins (IPR003347) in *M.oryzae,* and seven of them were predicted to functionally active as histone demethylases via Hidden-Markov profiling. Two genes, MGG_09841 and MGG_02045, were predicted to be fungal specific, and showed only higher similarity with *Fusarium graminearum* and *F. oxysporum* than other organisms. Furthermore, when analyzed with JmjC domain amino-acid sequences in ChromDB, they were not classified into other JmjC demethlyase groups, as well as in whole protein sequence level. Although one or two of LSD class demethylase exist in most organisms, JmjC class demethylases have been diverged in accordance with their various functions. The number of JmjC domain-containing proteins is 5 in yeast, 11 in *M. oryzae*, 20 in rice, 21 in *Arabidopsis*, and 30 in human. Yeast JmjC demethylases have less additional domains and biological functions than other organisms. For instance, in yeast, phenotypes of JmjC demethylase deletion mutatnt are not associated with cell development, and Jhd2, JARID group demethylase,

does not have BRIGHT/ARID and C5HC2-zf domains (Liang et al., 2007). It is thought that *M. oryzae* is in the middle of the divergence between yeast and human, because it has more JmjC domain-containing proteins than yeast and MGG_09186, belonging to JMJD2 group, was predicted to have two of alternative spliced form. Therefore, JmjC domain-containing proteins of *M. oryzae* show both conservation and divergence with other organisms.

In this study, it is revealed that *MoJMJ1* is essential for appressorium development through functional analysis. The germ-tubes of Δ*Mojmj1* showed swelling and hooking, and elongated excessively with branches in similarity with Δ*Mohox7* mutant. Kim et al. observed that germ-tube of Δ*Mohox7* accumulates lipid droplets during swelling and hooking, before switching to vegetative hyphal growth through Nile red staining, indicating that *MoHOX7* is not associated with recognition of environmental cues inducing appressorium formation, such as surface hardness, hydrophobicity, nutritional signal, and molecules from plant surface. Germ-tube of Δ*Mojmj1* appeared very similar with that of Δ*Mohox7*, and it is necessary to observe the accumulation of lipid droplets within germ-tubes of Δ*Mojmj1*. Also, Δ*Mohox7* mutnat forms non-melanized swellings and hooking from tip of hypha, suggesting that *MoHOX7* is required for development of appressoria, both from hyphae and germ-tubes. As Δ*Mojmj1* mutant showed melanized abnormal appressoria later 20 hours incubation, further experiments are required to clarify whether the abnormal appressoria of Δ*Mojmj1* is hypha-driven appressoria. Moreover, expression profile data indicated that *MoJMJ1* regulates genes of upstream regulator in $Ca^{2+}$ and cAMP-dependent signaling pathways. However, chemical complementation treating $CaCl_2$ and cAMP failed to recover defects in conidial

germination and appressorium development. It is thought that the reason is down-regulated expression of *MoHOX7* in Δ*Mojmj1*. *MoHOX7*, affected by *MoPLC1* and *MAC1*, is a downstream regulator in $Ca^{2+}$ and cAMP-dependent signaling pathways and none chemical complemented defects in appressorium development of Δ*Mohox7* (Kim et al., 2009). Taken together, *MoJMJ1* has important roles for appressorium development by regulating both upstream and downstream regulators in intracellular signal transduction cascades.

Conservation in domain architecture and sequence suggests that proteins have a similarity in function, and JmjC demethylase has a feature that compositions of Fe(II) and αKG-binding sites are diverse in according to substrate specificity. It was predicted that human JARID1C and D catalyze di- / trimethyl H3K4 according to prediction about domain structure and cofactor binding residues (Yamane et al., 2007), and the prediction was revealed to be right (Iwase et al., 2007; Lee et al., 2007). MoJMJ1 was analyzed with other protein sequences, which were already known to have functions as H3K4 demethylase, and it showed highly conserved cofactor binding residues in JmjC domain. It is well known that other additional domains are important for enzymatic activity in JARID group proteins. For instance, JARID1B/PLU-1 lost enzymatic activity when JmjN, BRIGHT/ARID, and C5HC2-zf domains were respectively deleted, as well as JmjC domain (Yamane et al., 2007). MoJMJ1 has also these indispensable JmjN, JmjC, BRIGHT/ARID, C5HC2-zf, and PHD domains, which is similar with human JARID1 orthologues in domain architecture and order. Overall, these results indicate that target substrates of MoJMJ1 are di- / trimethyl H3K4.

Δ*Mojmj1* showed defects in fungal developmental stages and pathogenicity, and it was

confirmed that MoJMJ1 regulates transcriptional expression of genes involved in the phenotypic defects. Di- / trimethyl H3K4 near transcription start site (TSS) of genes mean transcriptional active mark through altering chromatin structure to open, euchromatin. The result of qRT-PCR suggests that *MoAPS1* would be directly regulated by MoJMJ1, because fold change of *MoAPS1* was increased in condition of Δ*Mojmj1*. However, the other genes down-regulated in the condition, indicating that they are the target genes indirectly affected by MoJMJ1. It is explained by a possibility that gene activators and repressors could access to the open chromatin structure near the TSS of target genes by methyl groups at H3K4. By binding gene activators and repressors to nucleosome free-regions, the change of H3K4 methylation level perhaps leads to both transcriptional up- and down-regulation of target genes. Therefore, proper transcriptional regulation of MoJMJ1 is required for normal fungal development and pathogenicity.

Western blot analysis has been used for detection of enzymatic activity and substrate specificity in histone modifying enzyme researches. However, if the modifiers do not affect total protein level, there would be no significant difference in amounts of protein detected by Western blotting. Although knockdown of JARID1B/PLU-1 did not increase global H3K4 methylation levels, it resulted in increased trimethyl H3K4 levels at the region near transcriptional start site of specific target genes, as well as histone demethylase activity of JARID1B/PLU-1 was monitored by release of product, formaldehyde, made though demethylation mechanism (Yamane et al., 2007). The amounts of protein detected by H3K4 antibody were not increased in total proteins of Δ*Mojmj1*, suggesting that MoJMJ1 is not affect global level of trimethyl H3K4. Given the phenotypic defects of Δ*Mojmj1*, MoJMJ1 perhaps directly modulates trimethyl H3K4

level at several specific genes, not global H3K4 methylation level. Moreover, there is possibility that MoJMJ1 is not the major player for demethylation of H3K4. H3K4 demethylases are not only in JARID group, but also in LSD and JHDM1 groups of mammalian (Agger et al., 2008), and it was predicted that there are six of the other jmjC domain-containing proteins and one of gene encoding putative LSD class demethylase in *M. oryzae*. Further structural and enzymatic activity analysis regarding substrate specificity will hopefully provide information about demethylase inhibitors for rice blast control.

Complemented mutant strain, *MoJMJ1c*, was generated through transformation of native *MoJMJ1* construct into Δ*Mojmj1-1* protoplast in order to verify that phenotypic defects of Δ*Mojmj1* were resulted from deletion of *MoJMJ1*. *MoJMJ1c* restored all the defects in pre-penetration, but not in penetration and invasive growth, resulting in loss of pathogenicity. In an effort to resolve the problem, 5' upstream flanking region was lengthened from 1.25 kb to 2.1 kb. The regenerated complements were also unable to restore defects in penetration and invasive growth, indicating that promoter length is not the reason for the complementation problem. The method of PCR-based amplification was used to prepare constructs in complementation experiment, and it could give rise to point mutation in the constructs. However, it is thought that there is rarely potential for point mutation in the constructs. Three times of generating construct and transformation for complementation were independently conducted, and all complemented mutant strains showed the same results, recovering defects in pre-penetration, but not in penetration. Moreover, 3' flanking region in construct for generating Δ*Mojmj1* contained most of 5' UTR region of MGG_04877, locating downstream of *MoJMJ1* and predicted

to encode TFIID subunit 6 gene. To test complementation problem was resulted from abnormal expression of MGG_04877 in Δ*Mojmj1*, transcript of the gene was checked through RT-PCR. Result of the experiment revealed that transcription and splicing of the gene were intact, suggesting that MGG_04877 is not associated with phenotypic defects of Δ*Mojmj1*. A hypothesis to explain this discrepancy in complementation is that chromatin structure could be altered by H3K4 methylation level. Modulating the level of di- / trimethyl H3K4 by deletion of *MoJMJ1* would affect binding of reader proteins, resulting in recruiting or maintaining of chromatin remodelers. In this regard, Christensen et al. commented that most of JARID1 proteins participate in specific chromatin-remodeling complexes recruited to certain genomic areas (Christensen et al., 2007). Under the condition that chromatin state is altered and kept in Δ*Mojmj1*, complexes associated with transcriptional active or repressive state may complete each other when *MoJMJ1* is complemented. *MoJMJ1c* perhaps could not restore to switch over chromatin states that are important for gene expressions involved in normal penetration and invasive growth.

In summary, it was demonstrated that *MoJMJ1* encoding JmjC histone demethylase is required for fungal development and pathogenicity. Δ*Mojmj1* showed severe defects in fungal developmental stages, including development of conidiophores, normal conidial germ tubes, and appressorium formation, and *MoJMJ1* caused the defects through transcriptional regulation in fungal development-related genes. Furthermore, fungal pathogenesis is damaged by the developmental defects and transcriptional regulation. These results provide evidence that normal fungal development via transcriptional regulation by MoJMJ1 is essential for fungal pathogenicity. This study will help to

understand the epigenetic mechanisms involved in appressorium formation and contribute to novel strategy for rice blast control.

# LITERATURE CITED


Adhvaryu KK, Morris SA, Strahl BD, Selker EU, 2005. Methylation of histone H3 lysine 36 is required for normal development in Neurospora crassa. *Eukaryot Cell* 4, 1455-64.

Agger K, Christensen J, Cloos PA, Helin K, 2008. The emerging functions of histone demethylases. *Curr Opin Genet Dev* **18**, 159-68.

Agger K, Cloos PA, Rudkjaer L, *et al.*, 2009. The H3K27me3 demethylase JMJD3 contributes to the activation of the INK4A-ARF locus in response to oncogene- and stress-induced senescence. *Genes Dev* **23**, 1171-6.

Bok JW, Chiang YM, Szewczyk E, *et al.*, 2009. Chromatin-level regulation of biosynthetic gene clusters. *Nat Chem Biol* **5**, 462-4.

Choi J, Kim KS, Rho HS, Lee YH, 2011. Differential roles of the phospholipase C genes in fungal development and pathogenicity of Magnaporthe oryzae. *Fungal Genet Biol* **48**, 445-55.

Christensen J, Agger K, Cloos PA, *et al.*, 2007. RBP2 belongs to a family of demethylases, specific for tri-and dimethylated lysine 4 on histone 3. *Cell* **128**, 1063-76.

Chung H, Choi J, Park SY, Jeon J, Lee YH, 2013. Two conidiation-related Zn(II)2Cys6 transcription factor genes in the rice blast fungus. *Fungal Genet Biol* **61**, 133-41.

Dean R, Van Kan JA, Pretorius ZA, *et al.*, 2012. The Top 10 fungal pathogens in

molecular plant pathology. *Mol Plant Pathol* **13**, 414-30.

Desvoyes B, Sanchez MP, Ramirez-Parra E, Gutierrez C, 2010. Impact of nucleosome dynamics and histone modifications on cell proliferation during Arabidopsis development. *Heredity (Edinb)* **105**, 80-91.

Eissenberg JC, Lee MG, Schneider J, Ilvarsonn A, Shiekhattar R, Shilatifard A, 2007. The trithorax-group gene in Drosophila little imaginal discs encodes a trimethylated histone H3 Lys4 demethylase. *Nat Struct Mol Biol* **14**, 344-6.

Grimaldi B, Coiro P, Filetici P, *et al.*, 2006. The Neurospora crassa White Collar-1 dependent blue light response requires acetylation of histone H3 lysine 14 by NGF-1. *Mol Biol Cell* **17**, 4576-83.

Howard RJ, Valent B, 1996. BREAKING AND ENTERING: Host Penetration by the Fungal Rice Blast Pathogen Magnaporthe grisea.

Huarte M, Lan F, Kim T, *et al.*, 2007. The fission yeast Jmj2 reverses histone H3 Lysine 4 trimethylation. *J Biol Chem* **282**, 21662-70.

Iwase S, Lan F, Bayliss P, *et al.*, 2007. The X-linked mental retardation gene SMCX/JARID1C defines a family of histone H3 lysine 4 demethylases. *Cell* **128**, 1077-88.

Jeon J, Park SY, Chi MH, *et al.*, 2007. Genome-wide functional analysis of pathogenicity genes in the rice blast fungus. *Nat Genet* **39**, 561-5.

Jiang D, Yang W, He Y, Amasino RM, 2007. Arabidopsis relatives of the human lysine-specific Demethylase1 repress the expression of FWA and FLOWERING LOCUS C and thus promote the floral transition. *Plant Cell* **19**, 2975-87.

Khush GS, 2005. What it will take to feed 5.0 billion rice consumers in 2030. *Plant Mol Biol* **59**, 1-6.

Kim S, Park SY, Kim KS, *et al.*, 2009. Homeobox transcription factors are required for conidiation and appressorium development in the rice blast fungus Magnaporthe oryzae. *PLoS Genet* **5**, e1000757.

Klose RJ, Kallin EM, Zhang Y, 2006. JmjC-domain-containing proteins and histone demethylation. *Nat Rev Genet* **7**, 715-27.

Kooistra SM, Helin K, 2012. Molecular mechanisms and potential functions of histone demethylases. *Nat Rev Mol Cell Biol* **13**, 297-311.

Kouzarides T, 2007. Chromatin modifications and their function. *Cell* **128**, 693-705.

Lee MG, Norman J, Shilatifard A, Shiekhattar R, 2007. Physical and functional association of a trimethyl H3K4 demethylase and Ring6a/MBLR, a polycomb-like protein. *Cell* **128**, 877-87.

Lee YH, Dean R, 1993. CAMP Regulates lnfection Structure Formation in the Plant Pathogenic Fungus Magnaporthe grisea.

Leung H, Borromeo ES, A. BM, Notteghem JL, 1988. Genetic analtsis of virulence in the rice blast fungus Magnaporthe grigea.

Li B, Carey M, Workman JL, 2007. The role of chromatin during transcription. *Cell* **128**, 707-19.

Liang G, Klose RJ, Gardner KE, Zhang Y, 2007. Yeast Jhd2p is a histone H3 Lys4 trimethyl demethylase. *Nat Struct Mol Biol* **14**, 243-5.

Lu F, Cui X, Zhang S, Jenuwein T, Cao X, 2011. Arabidopsis REF6 is a histone H3 lysine 27 demethylase. *Nat Genet* **43**, 715-9.

Pasini D, Hansen KH, Christensen J, Agger K, Cloos PA, Helin K, 2008. Coordinated regulation of transcriptional repression by the RBP2 H3K4 demethylase and Polycomb-Repressive Complex 2. *Genes Dev* **22**, 1345-55.

Patsialou A, Wilsker D, Moran E, 2005. DNA-binding properties of ARID family proteins. *Nucleic Acids Res* **33**, 66-80.

Pedersen MT, Helin K, 2010. Histone demethylases in development and disease. *Trends Cell Biol* **20**, 662-71.

Quan TK, Hartzog GA, 2010. Histone H3K4 and K36 methylation, Chd1 and Rpd3S oppose the functions of Saccharomyces cerevisiae Spt4-Spt5 in transcription. *Genetics* **184**, 321-34.

Reyna NSY, Y., 2006. Molecular Analysis of the Rice MAP Kinase Gene Family in Relation to Magnaporthe grisea Infection. *Molecular Plant Microbe Biology*.

Scibetta AG, Santangelo S, Coleman J, *et al.*, 2007. Functional analysis of the transcription repressor PLU-1/JARID1B. *Mol Cell Biol* **27**, 7220-35.

Secombe J, Li L, Carlos L, Eisenman RN, 2007. The Trithorax group protein Lid is a trimethyl histone H3K4 demethylase required for dMyc-induced cell growth. *Genes Dev* **21**, 537-51.

Seward DJ, Cubberley G, Kim S, *et al.*, 2007. Demethylation of trimethylated histone H3 Lys4 in vivo by JARID1 JmjC proteins. *Nat Struct Mol Biol* **14**, 240-2.

Shi Y, 2007. Histone lysine demethylases: emerging roles in development, physiology and disease. *Nat Genet* **8**, 829-833.

Shi Y, Lan F, Matson C, *et al.*, 2004. Histone demethylation mediated by the nuclear

amine oxidase homolog LSD1. *Cell* **119**, 941-53.

Shi Y, Whetstine JR, 2007. Dynamic regulation of histone lysine methylation by demethylases. *Mol Cell* **25**, 1-14.

Shwab EK, Bok JW, Tribus M, Galehr J, Graessle S, Keller NP, 2007. Histone deacetylase activity regulates chemical diversity in Aspergillus. *Eukaryot Cell* **6**, 1656-64.

Silue D, Notteghem JL, Tharreau D, 1992. Evidence of a gene-for-gene relationship in the Oryza sativa-Magnaporthe grisea pathosystem.

Smith KM, Phatale PA, Sullivan CM, Pomraning KR, Freitag M, 2011. Heterochromatin is required for normal distribution of Neurospora crassa CenH3. *Mol Cell Biol* **31**, 2528-42.

Spannhoff A, Hauser AT, Heinke R, Sippl W, Jung M, 2009. The emerging therapeutic potential of histone methyltransferase and demethylase inhibitors. *ChemMedChem* **4**, 1568-82.

Strauss J, Reyes-Dominguez Y, 2011. Regulation of secondary metabolism by chromatin structure and epigenetic codes. *Fungal Genet Biol* **48**, 62-9.

Sun Q, Zhou DX, 2008. Rice jmjC domain-containing gene JMJ706 encodes H3K9 demethylase required for floral organ development. *Proc Natl Acad Sci U S A* **105**, 13679-84.

Tamaru HS, E. U., 2001. A histone H3 methyltransferase controls DNA methylation in Neurospora crassa. *Nature* **414**, 277-283.

Tanabe S, Nishizawa Y, Minami E, 2009. Effects of catalase on the accumulation of

H(2)O(2) in rice cells inoculated with rice blast fungus, Magnaporthe oryzae. *Physiol Plant* **137**, 148-54.

Tsukada Y, Fang J, Erdjument-Bromage H, *et al.*, 2006. Histone demethylation by a family of JmjC domain-containing proteins. *Nature* **439**, 811-6.

Upadhyay AK, Horton JR, Zhang X, Cheng X, 2011. Coordinated methyl-lysine erasure: structural and functional linkage of a Jumonji demethylase domain and a reader domain. *Curr Opin Struct Biol* **21**, 750-60.

Vu BV, Pham KT, Nakayashiki H, 2013. Substrate-induced transcriptional activation of the MoCel7C cellulase gene is associated with methylation of histone H3 at lysine 4 in the rice blast fungus Magnaporthe oryzae. *Appl Environ Microbiol* **79**, 6823-32.

Woloshuk CP, Sisler HD, Vigil EL, 1983. Action of the antipenetrant, tricyclazole, on appressoria of Pyricularia oryzae.

Xu JR, Hamer JE, 1996. MAP kinase and cAMP signaling regulate infection structure formation and pathogenic growth in the rice blast fungus Magnaporthe grisea. *Genes Dev* **10**, 2696-706.

Yamane K, Tateishi K, Klose RJ, *et al.*, 2007. PLU-1 is an H3K4 demethylase involved in transcriptional repression and breast cancer cell proliferation. *Mol Cell* **25**, 801-12.

# 요약 (국문초록)

히스톤의 번역 후 수식은 염색질 역학과 전사에 중요하다. 적절한 수식이 손상되면, 각각 식물과 동물에서 발달적 결함과 암을 야기할 수 있다. 진핵생물에서 후생유전학적 체제로서 히스톤 수식이 보편적임에도 불구하고, 곰팡이 병원성에서 히스톤 수식의 영향에 대한 연구는 이제 막 시작되는 단계이다. 본 연구에서는 식물병원성 곰팡이인 벼 도열병균의 히스톤 라이신 탈메틸화 효소로 추정되는 유전자들을 찾고 기능 분석을 하였다. 지금까지 히스톤 탈메틸화 효소는 LSD와 JmjC 도메인을 가지는 두 개의 분류군이 있는 것으로 밝혀져 있다. BLAST와 HMMER를 함께 사용하여, 도열병균에서 JmjC 도메인을 가진 히스톤 탈메틸화 효소를 암호화 하는 것으로 추정되는 7개의 유전자들을 찾았으며, 각각을 *MoJMJ1*부터 *MoJMJ7*이라고 명명하였다. 계통분류학적 분석을 통해, 이들 중 5개는 JARID, JMJD2, JHDM2, JmjC-only 도메인 그룹에 속하는 것으로 나타났다. JARID 그룹에 속하는 *MoJMJ1*의 삭제 변이체는 영양생장, 자가분해, 무성생식, 부착기 형성, 침입생장에 있어 결함이 생겨 기주인 벼에 병을 내지 못하는 표현형을 보였다. 또한, 삭제 변이체에서 부착기 형성에 관련한 유전자들과 *MoHOX*를 포함한 전사인자 유전자들의 발현이 유의미하게 변화하였다. *MoJMJ1* 유전자를 삭제 변이체에 재 삽입했을 때, 모든 결함을 회복한 것은 아니지만, 영양생장, 자가 분해, 무성생식, 부착기 형성의 표현형을 회복하는 것을 보아, *MoJMJ1*

에 의한 히스톤 탈메틸화의 조절이 곰팡이 발달과정과 부착기 형성에 중요함을 암시한다. 따라서, 본 연구에서 기능 분석한 히스톤 탈메틸화 효소 유전자의 연구 결과는 곰팡이의 병 발생에 있어 중요한 역할을 규명한 것으로서 충분한 가치가 있다고 판단된다.

주요어: 후생유전학, 히스톤 탈메틸화효소, 벼도열병균, 병원성, 부착기 발달

학번: 2012-21192